Journal of Zhejiang University SCIENCE A
ISSN 1673-565X (Print); ISSN 1862-1775 (Online)
www.zju.edu.cn/jzus; www.springerlink.com
E-mail: jzus@zju.edu.cn

Emission characteristics and combustion instabilities in an oxy-fuel swirl-stabilized combustor*

Guo-neng LI, Hao ZHOU†‡, Ke-fa CEN

(*State Key Laboratory of Clean Energy Utilization, Zhejiang University, Hangzhou 310027, China*)

†E-mail: zhouhao@cmee.zju.edu.cn

Received Apr. 21, 2008; revision accepted June 20, 2008

Abstract: This paper presents an experimental study on the emission characteristics and combustion instabilities of oxy-fuel combustions in a swirl-stabilized combustor. Different oxygen concentrations (X_{oxy}=25%~45%, where X_{oxy} is oxygen concentration by volume), equivalence ratios (φ=0.75~1.15) and combustion powers (CP=1.08~2.02 kW) were investigated in the oxy-fuel ($CH_4/CO_2/O_2$) combustions, and reference cases (X_{oxy}=25%~35%, $CH_4/N_2/O_2$ flames) were covered. The results show that the oxygen concentration in the oxidant stream significantly affects the combustion delay in the oxy-fuel flames, and the equivalence ratio has a slight effect, whereas the combustion power shows no impact. The temperature levels of the oxy-fuel flames inside the combustion chamber are much higher (up to 38.7%) than those of the reference cases. Carbon monoxide was vastly produced when X_{oxy}>35% or φ>0.95 in the oxy-fuel flames, while no nitric oxide was found in the exhaust gases because no N_2 participates in the combustion process. The combustion instability of the oxy-fuel combustion is very different from those of the reference cases with similar oxygen content. Oxy-fuel combustions excite strong oscillations in all cases studied X_{oxy}=25%~45%. However, no pressure fluctuations were detected in the reference cases when X_{oxy}>28.6% accomplished by heavily sooting flames which were not found in the oxy-fuel combustions. Spectrum analysis shows that the frequency of dynamic pressure oscillations exhibits randomness in the range of 50~250 Hz, therefore resulting in a very small resultant amplitude. Temporal oscillations are very strong with amplitudes larger than 200 Pa, even short time fast Fourier transform (FFT) analysis (0.08 s) shows that the pressure amplitude can be larger than 40 Pa.

Key words: Swirl, Oxy-fuel, Combustion instability, Pollutant emissions
doi:10.1631/jzus.A0820303 **Document code:** A **CLC number:** TK124; O614.3

INTRODUCTION

Oxy-fuel (CO_2/O_2) combustion technology is one of the promising solutions for controlling greenhouse gases of which CO_2 is by far the most important one in terms of the amount emitted. Nowadays power production contributes approximately one-third of the CO_2 released from the fossil fuel conversion process in the world. Power plants using fossil fuel and CO_2 recovery are believed to be the least costly alternative for CO_2-free power production although roughly one-fifth of the electricity produced will be lost by CO_2 separation and compression (Lyngfelt *et al.*, 2001). The semi-closed CO_2 gas turbine cycle gives an encouraging alternative for today's gas turbines (Bolland and Mathieu, 1998). When CO_2 is used in semi-closed turbines other than N_2, the thermodynamic properties of CO_2 are very different from those of N_2. It is necessary to study the characteristics of oxy-fuel combustions in swirl-stabilized combustors, such as the ignition delay, temperature level and combustion stability.

The oxy-fuel combustion in straight burners has been studied by several researchers. Kim *et al.*(2006; 2007a; 2007b) studied the NO production and flame

‡ Corresponding author

* Project supported by the National Natural Science Foundation of China (No. 50576081), Zhejiang Provincial Natural Science Foundation of China (No. R107532), Program for the New Century Excellent Talents in University (No. NCET-07-0761) and the Foundation for the Author of National Excellent Doctoral Dissertation of China (No. 200747)

length in 0.03~0.20 MW oxy-fuel combustors under different oxidizer velocities (0~80 m/s) and quarl angles (0°~15°). Boushaki *et al.*(2007) investigated the lift-off height of oxy-fuel flames and the flame spread angle in a separated-jet burner (a central natural gas jet surrounded by two oxygen jets) under different oxygen velocities (0~53.3 m/s) and angles of oxygen jets (0°~30°). The radiation aspect of oxy-fuel combustion was explored by Naik *et al.*(2003) and Andersson and Johnsson (2007). Naik *et al.*(2003) discussed the effects of radiation on NO formation in sooting oxy-fuel flames, and suggested that the radiative heat loss due to soot formation should be considered in predicting the peak flame temperature, and that soot significantly influences the amount of NO formation. Andersson and Johnsson (2007) analyzed the radiation characteristics of propane burning oxy-fuel combustion with different oxygen concentrations in gas mixtures (X_{oxy}=21% and 27%, where X_{oxy} is oxygen concentration by volume, and an air-fuel reference case). They found that the flame emisivities for the X_{oxy}=21% and 27% cases are much larger (up to 30%) than those of air-fuel flames. To our knowledge, little research has been conducted on the oxy-fuel combustion in swirl-stabilized combustors, which are more common in industry. This work will focus on the related measurement issues.

Combustion instability is a typical phenomenon in gas turbines no matter whether air-fuel combustion or oxy-fuel combustion is adopted (Dowling, 2000). The subject has been extensively explored. Hobson *et al.*(2000) measured the oscillating pressure in a number of 150 MW industrial gas turbines. Li H. *et al.*(2007) investigated the lean blowout in propane/air flames. Low-frequency temperature oscillations were found to increase sharply as the flames approach the inferior limit of the equivalence ratio. Giezendanner *et al.*(2005) employed laser-Doppler velocimetry, planar laser-induced fluorescence and laser Raman scattering to measure the axis velocity, temperature, heat release and dynamic pressure. Meier *et al.*(2007) proposed a feedback mechanism to account for the excitation of combustion instability. Reviews on the combustion instability in swirl-stabilized combustors were given by Keller (1995) and Syred (2006). Ditaranto and Hals (2006) investigated the combustion instability in a sudden expansion oxy-fuel burner. They proposed five resonant modes and found that the oxygen concentration in the oxidizer plays a key role in the triggering of instabilities. Unfortunately, little work has been reported on the combustion instability in oxy-fuel swirl-stabilized combustors.

This work experimentally investigated the burned gas components, temperature distribution and dynamic pressure behavior in well defined oxy-fuel combustion cases and reference cases in a swirl-stabilized combustor. Comparisons of temperature level and oscillating pressure between oxy-fuel flames and reference cases are presented. This study gives insight into the physical mechanism of oxy-fuel combustion technology, and helps to optimize the design of oxy-fuel swirl-stabilized combustors.

APPARATUS

The experimental system is shown in Fig.1. The swirl combustor is similar to the one used by Masri *et al.*(2004) while the bluff-body was removed and a central pilot jet was added. CH_4 and $O_2/CO_2/N_2$ are used as fuel and oxidizer separately. The mass flow rates are controlled precisely by two Alicat® and one D07® mass flow controllers (MFCs). The accuracy of the MFC is less than ±1.5%.

Seven temperature measuring holes are drilled along the combustion chamber, and the tip of the thermocouple is located at the center of the combustion chamber's cross-section. Type S thermocouples (T1-T7) with an accuracy of 0.25% full scale (FS) are used, and the distances between the injector exit and the thermocouple tips are 30 mm, 80 mm, 120 mm, 160 mm, 200mm, 300 mm and 580 mm downstream of the injector exit, sequentially. An HP 34970A unit and an HP 34908A block are used to collect the temperature signals. The HP 34970A unit has an accuracy of 6.5 bits and its largest sample rate is 250 Hz. Effects of radiation and convection on the thermocouple tips are not considered, so the measured temperatures only serve as reference temperatures in the discussion.

One pressure measuring hole is drilled at a location of 300 mm downstream of the injector exit on the opposite side of the temperature measuring holes. One CGY® dynamic pressure transducer is used, whose accuracy and dynamic range is ±0.5% FS and 20 kHz, respectively. Pressure signals are collected using an HP® 8401A VXI mainframe, a fast A/D module called

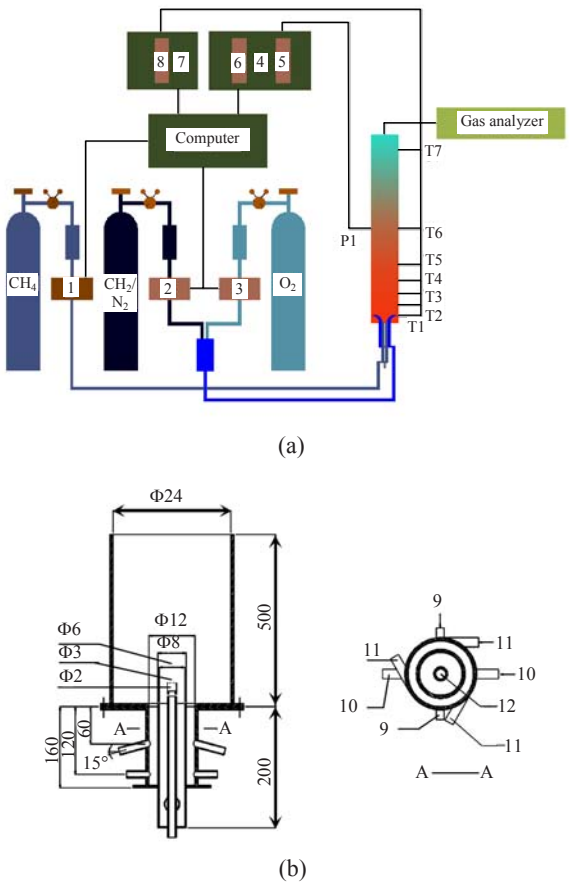

1, 2: Alicat mass flow controller (MFC); 3: D08 MFC; 4: HP VXI 8401A; 5: HP E1432A; 6: HP E8491A; 7: HP 34970A; 8: HP 34908A; 9: Fuel; 10: Primary air; 11: Secondary air; 12: Pilot fuel

Fig.1 Experimental system. (a) Experimental apparatus; (b) Experimental combustor (dimensions are in mm)

HP E1432A and a communicate module named HP E8491A. The sampling rate and accuracy of HP E1432A is 51200 Hz and 12 bits, respectively.

A continuous sampling program is developed using Agilent VEE®. The gas analyzer used is a Horiba PG-250, which utilizes Nondispersive Infrared measuring technique for CO_2 and CO, Chemiluminescence for NO_x, and Galvanic Cell for O_2. The accuracy of the gas analyzer is ±0.5% FS in all ranges of CO_2 and O_2 concentrations, and in the ranges for CO concentration larger than 1000×10^{-6} and for NO_x concentration above 100×10^{-6}. The accuracy is ±1.0% FS for CO concentration in ranges under 1000×10^{-6} and for NO_x concentration in ranges under 100×10^{-6}. The gas sampling location is 30 mm inside the combustion chamber upstream of the outlet. A series of experimental cases studied are shown in Table 1. The swirl number of the combustor is about 0.4 (Li G.N. *et al.*, 2007), which is deduced from the flow field simulated by FLUENT 6.1.22® with the definition of the swirl number as follows:

$$S_w = \frac{2\pi\rho\int_{R_i}^{R_j} WrUr\mathrm{d}r}{2\pi\rho\int_{R_i}^{R_j} UrUr\mathrm{d}r}, \quad (1)$$

where ρ is the air density, W is the tangential velocity, U is the axis velocity, and $R_i \rightarrow R_j$ is the integral radius. This swirl burner belongs to the category of low-swirl burner (LSB), which is widely used in the laboratory (Johnson *et al*., 2005).

Table 1 Experimental cases

Category No.	CH_4 (ml/s)	O_2 (ml/s)	CO_2 (ml/s)	N_2 (ml/s)	X_{O_2} (%)	φ	CP* (kW)
1	31.7	66.7	200.0		25	0.95	1.08
	31.7	66.7	155.5		30	0.95	1.08
	31.7	66.7	123.8		35	0.95	1.08
	31.7	66.7	100.0		40	0.95	1.08
	31.7	66.7	81.5		45	0.95	1.08
2	25.0	66.7	123.8		35	0.75	0.85
	28.3	66.7	123.8		35	0.85	0.96
	31.7	66.7	123.8		35	0.95	1.08
	35.0	66.7	123.8		35	1.05	1.08
	38.3	66.7	123.8		35	1.15	1.08
3	31.7	66.7	155.5		30	0.95	1.08
	39.6	83.3	194.5		30	0.95	1.35
	47.5	100.0	233.3		30	0.95	1.62
	59.4	125.0	291.7		30	0.95	2.02
4	31.7	66.7		200.0	25	0.95	1.08
	31.7	66.7		155.5	30	0.95	1.08
	31.7	66.7		123.8	35	0.95	1.08
	47.5	100.0		300.0	25	0.95	1.62
	47.5	100.0		233.3	30	0.95	1.62

*CP: combustion power is calculated from the heat value of methane, 34000 kJ/m^3

RESULTS AND DISCUSSIONS

Temperature level and emission characteristics

Temperature distributions along the axis of the combustion chamber in various cases are shown in Fig.2. Combustion delay (Combustion delay is defined as the time from the moment that the fuel is injected from the fuel nozzle to the moment that the highest mixture temperature is reached) as well as the

temperature level near the injector exit is influenced seriously by the oxygen concentration as shown in Fig.2a. Fig.2a indicates that the highest measured temperature in the case where X_{oxy}=45% is 336 K higher than that in the case where X_{oxy}=25% corresponding to approximately 24.5% improvement. In the case where X_{oxy}=25% a highest measured temperature of 1376 K appears at the location of 80 mm downstream of the injector exit. The higher temperature level in the case where X_{oxy}=45% is caused by the reduced amount of CO_2, accordingly less heat is absorbed in the flame zone. Both X_{oxy}=25% and X_{oxy}=30% cases exhibit a large negative temperature gradient from 80 mm to 200 mm downstream of the injector exit, which represents the location of the flame front. At this location, the temperatures in the cases of X_{oxy}=35%, X_{oxy}=40%, and X_{oxy}=45% start to decrease already from the first measuring point, and no parabolic shape is found in the temperature profile, although a weak trend in parabolic-like temperature profile may exist between 0 mm and 30 mm downstream of the injector exit. In other words, the oxygen concentration in the oxidizer is the key parameter in controlling the combustion delay of oxy-fuel flames, e.g., a lower oxygen concentration in the oxidizer will delay the burnout of oxy-fuel combustion.

The equivalence ratio has a slight effect on the combustion delay as shown in Fig.2b, e.g., the flame fronts of both φ=1.05 and φ=1.15 cases are at 80 mm downstream of the injector exit, while the cases of φ=0.75, φ=0.85 and φ=0.95 have no parabolic-like temperature profiles. It should be noted that all the cases shown in Fig.2b are assigned a fixed oxygen concentration of 35%. Cases where φ=1.05 and φ=1.15 will not be used in practical devices, because pollutant emissions are vastly produced in these fuel-rich cases, which will be discussed later. As a consequence, the influence of equivalence ratio makes only a minor contribution to the combustion delay in oxy-fuel flames.

Combustion power (CP) has no effect on the combustion delay as shown in Fig.2c. The temperature level in the *CP*=2.02 kW case is approximately 16.5% higher on average than that of the *CP*=1.08 kW case, but the flame fronts of all the cases with a fixed oxygen concentration of 30% are at 80 mm downstream of the injector exit. The largest combustion power is 87% higher than that of the smallest one, yet no shift in the position of the flame front is detected. Therefore, the effect of combustion power on the combustion delay could be excluded.

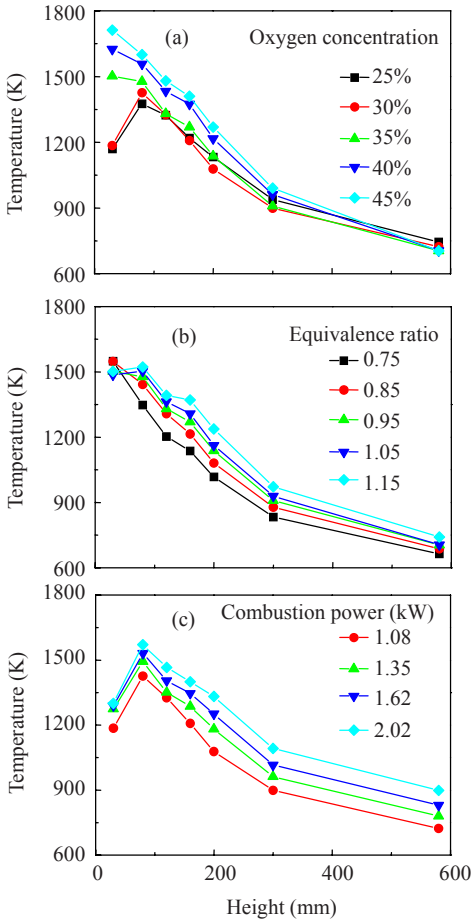

Fig.2 Effects of (a) oxygen content, (b) equivalence ratio (X_{oxy}=30%) and (c) combustion power (X_{oxy}=35%) on temperature distribution

Fig.3 shows the comparison of the temperature level between oxy-fuel combustions and reference flames. The temperature level of the CO_2/O_2 case is 38.7% higher on average than that of N_2/O_2 case when X_{oxy}=25% while this improvement is 22.2% when X_{oxy}=30%. The much higher average temperature level of oxy-fuel combustions results from the much higher gas emissivity of oxy-fuel burned gases than that of reference flames. According to Andersson and Johnsson (2007), the emissivity of oxy-fuel burned gases can be 30% larger than that of a reference case with similar combustion power and oxygen concentration in the oxidizer. As shown in Fig.3, the slope coefficients of the temperature behind the flame front in oxy-fuel flames are smaller than those of reference

cases. It is interesting to find that the difference levels (i.e., 22.2% to 38.7%) between case X_{oxy}=30% and case X_{oxy}=25% are quite different, corresponding to a difference of 74%. The reason lies in the soot radiation of the reference flame with X_{oxy}=30% which will be discussed later. Another interesting phenomenon is that the combustion delay is very different between oxy-fuel combustions and reference flames, e.g., the flame front of oxy-fuel flames is at 80 mm downstream of the injector exit, whereas this is not so for the reference cases with similar oxygen concentration in the oxidizer. This phenomenon is caused by the much higher density and heat capacity of CO_2 compared to N_2.

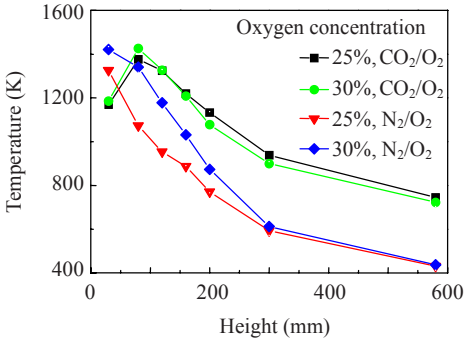

Fig.3 Comparison of temperature level between CH_4/CO_2/O_2 flames and CH_4/N_2/O_2 flames with methane flow rates of 31.7 ml/s

Fig.4 shows the measured exhaust gas compositions of oxy-fuel combustions. As shown in Fig.4a, the unburned oxygen concentration in the exhaust gases decreases with the increasing equivalence ratio. The reason for this phenomenon lies in the fact that the mixture is approaching the stoichiometric situation. The unburned oxygen concentration decreases firstly with the increasing oxygen concentration in the oxidizer, followed by an increase in the case where X_{oxy}=45% which is shown in Fig.4b. The underlining mechanism is that the mixture with higher oxygen concentration has a larger flame speed (Ditaranto and Hals, 2006), and becomes combustible more easily. When the oxygen concentration is too high (X_{oxy}=45%) CH_4/CO_2/O_2 flame has a much higher combustion temperature, which excites much stronger combustion instability, causing the unburned oxygen concentration to increase. As shown in Fig.4, CO concentration in the exhaust gases remains at a low level when $\varphi \leq 0.95$ and $X_{oxy} \leq 35\%$ while the CO concentration increases sharply when φ>0.95 and X_{oxy}>35% due to the uncompleted combustion of methane. From the fuel saving aspect, oxy-fuel burners should be run with an equivalence ratio of less than 0.95, which is shown in Fig.4a, because the amount of CO concentration is at a low level under these conditions. A higher temperature level can be obtained when the oxygen concentration in the oxidizer increases, which is shown in Fig.2a, yet an too large oxygen concentration will cause a mass of CO as shown in Fig.4b. So an oxy-fuel burner like the one used in this work should be operated with an oxygen concentration not larger than 30%.

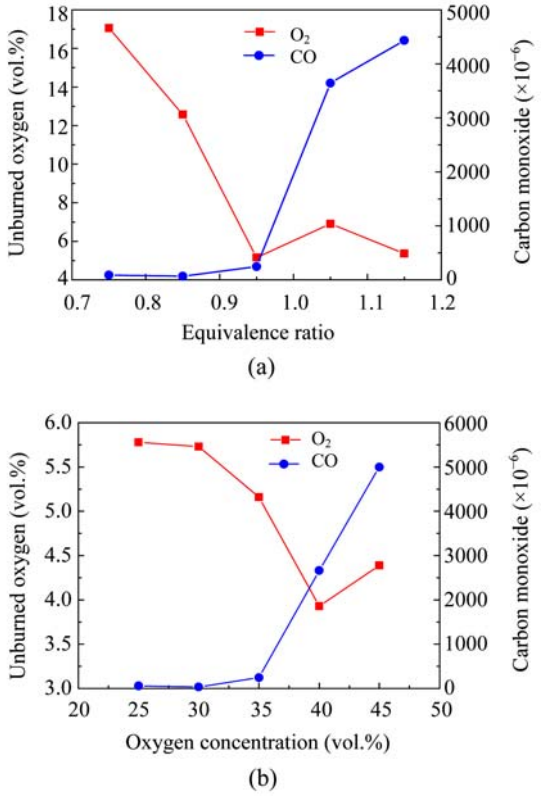

Fig.4 Measured concentrations of unburned oxygen and carbon monoxide in the oxy-fuel flames. (a) Different equivalence ratios while X_{oxy}=30%, oxygen flow rate is 66.7 ml/s, and carbon dioxide flow rate is 123.8 ml/s; (b) Different oxygen concentrations while φ=0.95, methane flow rate is 31.7 ml/s, and oxygen flow rate is 66.7 ml/s

Fig.5 shows the comparison of NO_x concentration between oxy-fuel combustions and reference cases. No nitric oxide is produced in oxy-fuel combustions because no nitrogen participates in the reaction process, whereas the NO_x concentration increases sharply with the oxygen concentration in the oxidizer

in reference flames. Apart from the original purpose of recovering the greenhouse gas CO_2, oxy-fuel combustion technology provides a good solution for the NO_x-free energy conversion process.

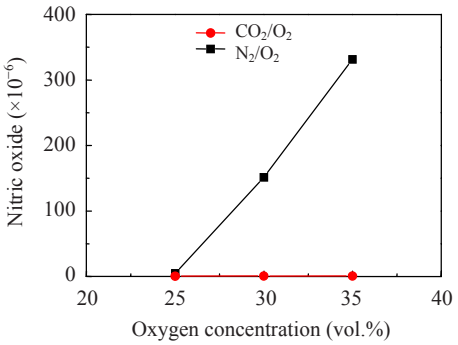

Fig.5 Comparison of the concentration of nitric oxide between $CH_4/CO_2/O_2$ flames and $CH_4/N_2/O_2$ flames with methane flow rates of 31.7 ml/s

Combustion instability

Fig.6 illustrates the oscillating pressure waveforms of both oxy-fuel combustions and reference cases with φ=0.95 and a methane flow rate of 31.7 ml/s. Combustion instability is excited both in the oxy-fuel combustions and reference cases with X_{oxy}=25%. The oscillating pressure waves in these cases fluctuate arbitrarily and in disorder. Spectrum analysis was carried out, and results will be discussed in the following paragraph. It is very interesting to find that the fluctuating pressure waves in the reference case with X_{oxy}=30% disappear as shown in Fig.6b, accomplished by a heavily sooting flame, whereas the situation for the oxy-fuel case with similar oxygen concentration is not the same. The oscillating pressure is amplified into larger amplitude fluctuations compared to that in the X_{oxy}=25% oxy-fuel case. The phenomenon was not reported previously and needs further study. The soot in the reference case with X_{oxy}=30% participates in the radiation heat transfer, causing a higher temperature level in the whole combustion chamber, as shown in Fig.3. Previous experimental study (Brookes and Moss, 1999) revealed that the radiation emission in sooting methane flames is stronger than that in non-sooting methane flames, and the radiation intensity caused by soot particles is larger than that caused by CO_2 and H_2O when the mean soot volume fraction is larger than 4.0×10^{-8}. In future works, the mean soot volume fraction and the diameter distribution of soot particles should be measured. Repeated experiments were carried out carefully to confirm that the critical oxygen concentration for reference sooting flames is approximate 28.6% for the combustor in this work. It is not certain whether or not the soot suppresses the self-excited oscillating pressure waves inside the combustion chamber. The two-phase gas-soot fluid produced in the reference case with X_{oxy}=30% may absorb the fluctuations excited by the unsteady combustion of methane, yet no proofs were measured in this study. Previous experimental study (Saito *et al*., 1998) showed that soot could be suppressed by forcing acoustic oscillations with the appropriate acoustic amplitude and frequency. Further study should be carried out in the future to investigate changes in the behavior of a self-excited oscillating flame due to the presence of soot. As shown in Fig.6, the oscillating pressure amplitude in the oxy-fuel cases increases with the increasing oxygen concentration in the oxidizer, showing a temporal amplitude larger than 200 Pa, which corresponds to the amplitude excited in some 150 MW gas turbines (Hobson *et al.*, 2000). This change law is caused by the higher temperature level in the oxy-fuel cases with a higher oxygen content, especially the zone near the injector exit, which is shown in Fig.2a.

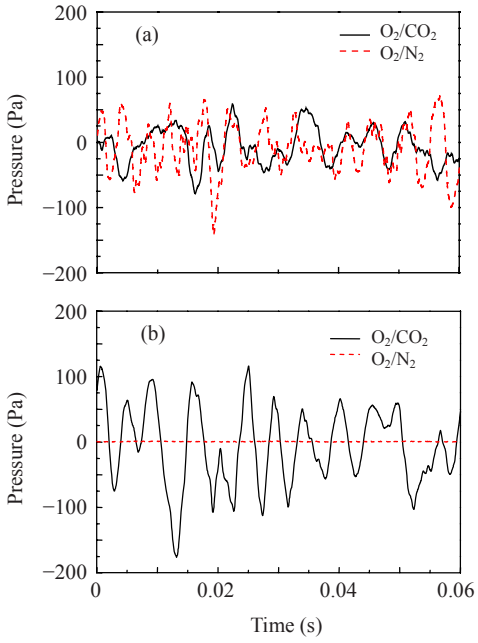

Fig.6 Oscillating pressure waveforms of cases with φ=0.95 and methane flow rates of 31.7 ml/s. (a) X_{oxy}=25%; (b) X_{oxy}=30%

Spectrum analysis of the oxy-fuel case with X_{oxy}=30% and a methane flow rate of 31.7 ml/s is shown in Fig.7. Also as shown in Fig.7, six continuous data blocks with fast Fourier transform (FFT) size of 2048 were used to be processed for detailed information in the time coordinate. This idea is similar to the theory adopted by the joint-time-frequency analysis (JTFA) method (Qian and Chen, 1999). These results are shown in Figs.7a and 7b, while Fig.7c shows a whole FFT analysis of continuous 128000 data points. It is noted that the whole FFT analysis gives a much lower amplitude of the pressure waves, e.g., about 7 Pa (111 dB, reference pressure is 2×10^{-5} Pa) at position of 200 Hz, whereas the short time (0.08 s) FFT result gives a much larger fluctuating amplitude, e.g., above 40 Pa (126 dB) at position of 125 Hz in the FFT1 analysis as shown in Fig.7a. This finding reveals the fact that the oscillating pressure in the swirl-stabilized combustor studied in this work is time-varying and frequency-varying pressure waveforms, but FFT takes all the signals to be time-varying and frequency-constant signals. As a consequence, the sound energy sprays out in a wide frequency range of 50~250 Hz, as shown in Fig.7. Therefore, the whole FFT analysis gives an amplitude not larger than 8 Pa. Some main peaks include 88 Hz, 125 Hz, 175 Hz and 200 Hz, some of which arise in one short time FFT result or another, and all these short time FFT results are superimposed to give a similar result to that of the whole FFT analysis. In future studies on the combustion instability in swirl-stabilized combustors, JTFA is recommended to detect the information in both the time and frequency spaces.

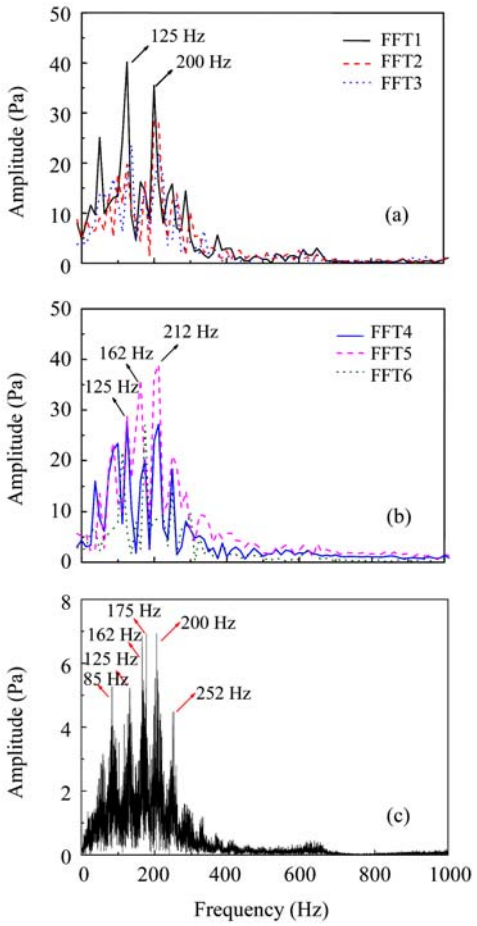

Fig.7 Spectrum analysis of the oxy-fuel case with X_{oxy}=30% and methane flow rates of 31.7 ml/s. (a) and (b) Results of 6 continuous data blocks with FFT size of 2048; (c) Result of continuous 128000 data points

CONCLUSION

Oxy-fuel combustions have been studied in a swirl-stabilized combustor with a swirl number of about 0.4. Various experimental cases have been explored, and necessary reference cases ($CH_4/N_2/O_2$ flames) were covered. Some concluding remarks can be made as follows.

(1) The combustion delay in oxy-fuel combustions is mainly controlled by the oxygen concentration in the oxidant stream. The equivalence ratio makes a minor contribution to the combustion delay, whereas the combustion power is found to have no impact.

(2) Carbon monoxide was vastly produced when X_{oxy}>35% or φ>0.95 in oxy-fuel flames. No nitric oxide in the exhaust gases was found since no nitrogen participates in the combustion process, whereas the concentration of nitric oxide increases sharply with the same oxygen concentration in $CH_4/N_2/O_2$ flames.

(3) The feature of combustion instability in oxy-fuel combustions is very different from that in the reference cases with similar oxygen concentration, e.g., pressure fluctuations disappeared in the reference cases when X_{oxy}>28.6% accomplished with a heavily sooting flame which was not found in oxy-fuel combustions. Spectrum analysis shows that the oscillating frequency exhibits randomness in the range of 50~250 Hz, indicating that the sound energy sprays out in a wide frequency range which results in a very small resultant amplitude (less than 8 Pa). In future studies

on combustion instability in swirl-stabilized combustors, JTFA is recommended to detect the information in both the time and frequency spaces.

References

Andersson, K., Johnsson, F., 2007. Flame and radiation characteristics of gas-fired O_2/CO_2 combustion. *Fuel*, **86**(5-6):656-668. [doi:10.1016/j.fuel.2006.08.013]

Bolland, O., Mathieu, P., 1998. Comparison of two CO_2 removal options in combined cycle power plants. *Energy Conversion and Management*, **39**(16-18):1653-1663. [doi:10.1016/S0196-8904(98)00078-8]

Boushaki, T., Sautet, J.C., Salentey, L., Labegorre, B., 2007. The behavior of lifted oxy-fuel flames in burners with separated jets. *International Communications in Heat and Mass Transfer*, **34**(1):8-18. [doi:10.1016/j.icheatmasstransfer.2006.09.008]

Brookes, S.J., Moss, J.B., 1999. Measurements of soot production and thermal radiation from confined turbulent jet diffusion flames of methane. *Combustion and Flame*, **116**(1-2):49-61. [doi:10.1016/S0010-2180(98)00027-3]

Ditaranto, M., Hals, J., 2006. Combustion instabilities in sudden expansion oxy-fuel flames. *Combustion and Flame*, **146**(3):493-512. [doi:10.1016/j.combustflame.2006.04.015]

Dowling, A.P., 2000. The Challenges of Lean Premixed Combustion. Proceeding of the International Gas Turbine Congress, Tokyo.

Giezendanner, R., Weigand, P., Duan, X.R., Meier, W., Meier, U., Aigner, M., Lehmann, B., 2005. Laser-based investigations of periodic combustion instabilities in a gas turbine model combustor. *Journal of Engineering for Gas Turbines and Power*, **127**(3):492-496. [doi:10.1115/1.1850498]

Hobson, D.E., Fackrell, J.E., Hewitt, G., 2000. Combustion instabilities in industrial gas turbines-measurements on operating plant and thermoacoustic modeling. *Journal of Engineering for Gas Turbines and Power*, **122**(3):420-428. [doi:10.1115/1.1287238]

Johnson, M.R., Littlejohn, D., Nazeer, W.A., Smith, K.O., Cheng, R.K., 2005. A comparison of the flowfields and emissions of high-swirl injectors and low-swirl injectors for lean premixed gas turbines. *Proceedings of the Combustion Institute*, **30**(2):2867-2874. [doi:10.1016/j.proci.2004.07.040]

Keller, J.J., 1995. Thermoacoustic oscillations in combustion chambers of gas turbines. *AIAA Journal*, **33**(12):2280-2287. [doi:10.2514/3.12980]

Kim, H.K., Kim, Y., Lee, S.M., Ahn, K.Y., 2006. Emission characteristics of the 0.03 MW oxy-fuel combustor. *Energy & Fuel*, **20**(5):2125-2130. [doi:10.1021/ef050232p]

Kim, H.K., Kim, Y., Lee, S.M., Ahn, K.Y., 2007a. Studies on combustion characteristics and flame length of turbulent oxy-fuel flames. *Energy & Fuel*, **21**(3):1459-1467. [doi:10.1021/ef060346g]

Kim, H.K., Kim, Y., Lee, S.M., Ahn, K.Y., 2007b. NO reduction in 0.03-0.2 MW oxy-fuel combustor using flue gas recirculation technology. *Proceedings of the Combustion Institute*, **31**(2):3377-3384. [doi:10.1016/j.proci.2006.08.083]

Li, G.N., Zhou, H., Cen, K.F., 2007. Experimental Study of Thermoacoustic Instability under Different Swirl Intensities. Challenges Power Engineering and Environment, Zhejiang University Press & Springer, Hangzhou, p.670-676.

Li, H., Zhou, X., Jeffries, J.B., Hanson, R.K., 2007. Sensing and control of combustion instabilities in swirl-stabilized combustors using Diode-laser absorption. *AIAA Journal*, **45**(2):390-398. [doi:10.2514/1.24774]

Lyngfelt, A., Leckner, B., Mattisson, T., 2001. A fluidized-bed combustion process with inherent CO_2 separation: application of chemical-looping combustion. *Chemical Engineering Science*, **56**(10):3101-3113. [doi:10.1016/S0009-2509(01)00007-0]

Masri, A.R., Kalt, P.A., Barlow, R.S., 2004. The compositional structure of swirl-stabilized turbulent nonpremixed flames. *Combustion and Flame*, **137**(1-2):1-37. [doi:10.1016/j.combustflame.2003.12.004]

Meier, W., Weigand, P., Duan, X.R., Giezendanner-Thoben, R., 2007. Detailed characterization of the dynamics of thermoacoustic pulsations in a lean premixed swirl flames. *Combustion and Flame*, **150**(1-2):2-26. [doi:10.1016/j.combustflame.2007.04.002]

Naik, S.V., Laurendeau, N.M., Cooke, J.A., Smooke, M.D., 2003. Effect of radiation on nitric oxide concentration under sooting oxy-fuel conditions. *Combustion and Flame*, **134**(4):425-431. [doi:10.1016/S0010-2180(03)00140-8]

Qian, S., Chen, D., 1999. Joint time frequency analysis. *IEEE Signal Processing Magazine*, **16**(2):52-67. [doi:10.1109/79.752051]

Saito, M., Sato, M., Nishimura, A., 1998. Soot suppression by acoustic oscillated combustion. *Fuel*, **77**(9-10):973-978. [doi:10.1016/S0016-2361(97)00286-X]

Syred, N., 2006. A review of oscillation mechanisms and the role of the processing vortex core (PVC) in swirl combustion systems. *Progress in Energy and Combustion Science*, **32**(2):93-161. [doi:10.1016/j.pecs.2005.10.002]